Published in final edited form as:
Development. 2008 December ; 135(23): 3959–3968. doi:10.1242/dev.025304.

The Mn1 transcription factor acts upstream of *Tbx22* and preferentially regulates posterior palate growth in mice

Wenjin Liu[a], **Yu Lan**[a], **Erwin Pauws**[b], **Magda A. Meester-Smoor**[c], **Philip Stanier**[b], **Ellen C. Zwarthoff**[c], and **Rulang Jiang**[a,*]

[a]*Department of Biomedical Genetics and Center for Oral Biology, University of Rochester School of Medicine and Dentistry, Rochester, NY 14642, USA* [b]*Institute of Child Health, University College London, London, WC1N 1EH, United Kingdom* [c]*Department of Pathology, Josephine Nefkens Institute, Erasmus MC, Rotterdam, The Netherlands.*

Summary

The mammalian secondary palate exhibits morphological, pathological, and molecular heterogeneity along the anterior-posterior axis. Although the cell proliferation rates are similar in the anterior and posterior regions during palatal outgrowth, previous studies have identified several signaling pathways and transcription factors that specifically regulate the growth of the anterior palate. In contrast, no factor has been shown to preferentially regulate posterior palatal growth. Here we show that mice lacking the transcription factor Mn1 have defects in posterior but not anterior palatal growth. We show that *Mn1* mRNA exhibits differential expression along the anterior-posterior axis of the developing secondary palate, with preferential expression in the middle and posterior regions during palatal outgrowth. Extensive analyses of palatal gene expression in wild-type and $Mn1^{-/-}$ mutant mice identified *Tbx22*, the mouse homolog of the human X-linked cleft palate gene, as a putative downstream target of Mn1 transcriptional activation. *Tbx22* exhibits a similar pattern of expression with that of Mn1 along the anterior-posterior axis of the developing palatal shelves and its expression is specifically down-regulated in $Mn1^{-/-}$ mutants. Moreover, we show that Mn1 activated reporter gene expression driven by either the human or mouse *Tbx22* gene promoters in co-transfected NIH3T3 cells. Overexpression of *Mn1* in NIH3T3 cells also increased endogenous *Tbx22* mRNA expression in a dose-dependent manner. These data indicate that Mn1 and Tbx22 function in a novel molecular pathway regulating mammalian palate development.

Keywords

cleft palate; Mn1; palate development; anterior-posterior patterning; Tbx22

Introduction

The *meningioma-1* (*MN1)* gene was first identified as the gene disrupted by a balanced chromosomal translocation that caused meningioma, a benign brain tumor (Lekanne Deprez et al., 1995). *MN1* encodes a protein of 1,319 amino acids, with no homology to any known functional domains, but the gene is evolutionarily conserved from *Drosophila* to human (Lekanne Deprez et al., 1995). While its relation to meningioma remains unclear since no mutations or deletions of the *MN1* gene have been found in other meningioma patients, the *MN1* gene has been shown to play important roles in acute myeloid leukemia (AML)

*Author for correspondence (email: Rulang_Jiang@urmc.rochester.edu).

pathogenesis (reviewed by Grosveld, 2007). MN1 is the target of a recurrent chromosomal translocation, t(12;22)(p13;q12), associated with human AML (Buijs et al., 1995). The translocation fuses the *MN1* gene with the *TEL* gene that encodes an ETS family DNA-binding transcription factor. Both *in vitro* and *in vivo* studies showed that the MN1-TEL fusion protein is oncogenic and that the transforming activity of the fusion protein depended on the N-terminal 500 amino acid residues of the MN1 protein (Buijs et al., 2000; Kawagoe and Grosveld, 2005a; Kawagoe and Grosveld, 2005b; Carella et al., 2006). In addition, *MN1* is overexpressed in many AML patients associated with other chromosomal abnormalities and in some AML patients without karyotype abnormalities (Ross et al., 2004; Valk et al., 2004; Du et al., 2005; Heuser et al., 2006; reviewed by Grosveld, 2007). Moreover, overexpression of *MN1* in the bone marrow caused malignant myeloid disease in mice (Carella et al., 2007). While the molecular mechanisms involving *MN1* in AML pathogenesis remains to be elucidated, several biochemical studies have showed that MN1 can function as a transcriptional coactivator of the nuclear hormone receptors for retinoic acid or vitamin D (van Wely et al., 2003; Sutton et al., 2005). MN1 has also been shown to interact with the transcriptional coactivators p300/CBP and RAC3 and to mediate transcriptional activation via CACCC-rich DNA sequences (van Wely et al., 2003; Meester-Smoor et al., 2007). Thus, in addition to involvement in AML, MN1 may interact with other transcription factors to regulate cell proliferation and cell differentiation during mammalian development.

To further investigate the roles of MN1 in oncogenesis and development, Meester-Smoor et al. (2005) generated mice with a targeted deletion in the orthologous *Mn1* gene. Although the mutant mice did not exhibit any increased incidence of tumor formation, all $Mn1^{-/-}$ homozygous mutant mice died shortly after birth and exhibited severe craniofacial developmental defects, including cleft palate, and some $Mn1^{+/-}$ heterozygous mutant mice also had cleft palate (Meester-Smoor et al., 2005). In mice, as in humans, the secondary palate develops from bilateral outgrowth on the oral side of the developing maxillary processes. The palatal processes initially grow vertically flanking the developing tongue. At a specific developmental time the bilateral palatal shelves reorient to the horizontal position above the tongue, grow toward and fuse with each other at the midline to form the intact roof of the oral cavity (Ferguson, 1988). Cleft palate may result from disturbances in the growth, elevation, or fusion of the palatal shelves. Gene inactivation studies in mice have demonstrated that many genes play essential roles in palatal shelf growth, including *Bmp4*, *Bmpr1a*, *Fgf10*, *Fgfr2b*, *Msx1*, *Osr2*, *Shox2*, and *Tgfbr2*, indicating that multiple molecular pathways interact to regulate palate development (Zhang et al., 2002; Han et al., 2003; Ito et al., 2003; Lan et al., 2004; Rice et al., 2004; Alappat et al., 2005; Liu et al. 2005; Yu et al., 2005). Moreover, since palate development occurs concurrently with significant growth and morphogenesis of the craniofacial complex, gross defects in structures outside of the palatal shelves may sometime hinder palatal shelf elevation or contact, resulting in cleft palate (reviewed by Chai and Maxson, 2006). To understand the roles of Mn1 in palate development, we have characterized its expression patterns during normal palate development and have identified a primary role for Mn1 in differential regulation of palatal growth along the anterior-posterior axis.

The mammalian secondary palate is divided anatomically into the anterior bony region (hard palate) and the posterior muscular region (soft palate) (Sperber, 2002). Cleft palate defects affecting the entire palate (complete cleft of the secondary palate) or either the anterior or posterior regions (incomplete cleft of the secondary palate) have been well documented (reviewed by Hilliard et al., 2005). Consistent with the morphological and pathological differences in the anterior and posterior palate, recent studies have clearly demonstrated that there is molecular heterogeneity along the anterior-posterior axis of the developing secondary palate (reviewed by Hilliard et al., 2005; Li and Ding, 2007). During early palate development, expression of several critical signaling molecules and transcription factors, including Bmp4, Fgf10, Msx1 and Shox2, is highly restricted along the anterior-posterior axis. Expression of

Bmp4 and *Msx1* is restricted to the most anterior 25% whereas *Fgf10* and *Shox2* are expressed in the anterior half of the developing palatal shelves, up to the level of the first molar tooth buds, prior to palatal fusion (Zhang et al., 2002; Alappat et al., 2005; Yu et al., 2005; Hilliard et al., 2005; Li and Ding, 2007). Fgf10 signals through the Fgfr2b receptor to regulate palatal epithelial cell proliferation and survival (Rice et al., 2004; Alappat et al., 2005). Bmp4 and Msx1 appeared to function in a positive feedback loop to regulate mesenchymal proliferation in the anterior palate (Zhang et al., 2002). Interestingly, exogenous Bmp4 induced *Msx1* expression and cell proliferation in the anterior but not in the posterior palatal mesenchyme in explant culture assays (Zhang et al., 2002; Hilliard et al., 2005). *Shox2* is also required for growth of the anterior palate and mice lacking *Shox2* exhibited incomplete cleft within the anterior palate while the mutant posterior palate fused normally (Yu et al., 2005). Although the anterior and posterior palatal regions exhibit similar growth rates during palatal outgrowth (Zhang et al., 2002; Li and Ding, 2007), however, no factor has been reported to preferentially regulate the growth of the posterior palate. The *Meox2* homeobox gene has been reported as being expressed in the posterior but not in the anterior palatal shelves in certain strains of mice (Jin and Ding, 2006; Li and Ding, 2007). Some, but not all, *Meox2* mutant mice exhibited cleft palate, but they did not have defects in palatal shelf growth and their cleft palate defect appeared to result from postfusion rupture (Jin and Ding, 2006). In this report, we show that Mn1 preferentially regulates the growth of the posterior palate in mice. In addition, we show that palatal expression of *Tbx22*, in which mutations cause X-linked cleft palate and ankyloglossia (CPX) in humans (Braybrook et al., 2001; 2002), is specifically regulated by Mn1. These data provide novel insights into the molecular mechanisms regulating the regional growth and patterning of the secondary palate.

Materials and methods

Mice

Mice carrying the targeted mutation in *Mn1* have been described previously (Meester-Smoor et al., 2005). *Mn1*$^{+/-}$ mice were maintained in the FVB congenic background and were intercrossed to generate homozygous mutant embryos for experimental analysis. Wild-type C57BL/6J and CD-1 mice were also used for in situ hybridization analysis of *Mn1* and *Tbx22* mRNA expression during palate development.

In situ hybridization and histological analyses

Embryos at different stages were dissected, fixed in 4% paraformaldehyde (PFA) in PBS overnight at 4°C. Whole mount in situ hybridization was performed as described previously (Lan et al., 2001). For section in situ hybridization, PFA-fixed embryos were dehydrated through graded alcohols and embedded in paraffin, sectioned at 7 μm thickness, followed by prehybridization processing and by hybridization with digoxigenin-labeled cRNA probes as described previously (Zhang et al., 1999).

For histology, embryos were collected at predetermined stages, fixed in either Bouin's fixative or 4% PFA overnight, dehydrated through graded ethanol, embedded in paraffin wax and sectioned at 7 μm thickness, followed by staining with haematoxylin and eosin.

Analyses of cell proliferation and cell apoptosis

Cell proliferation was measured by BrdU incorporation assays or detection of Ki67. For BrdU incorporation assays, timed mating was set up between *Mn1*$^{+/-}$ heterozygous mice and pregnant female mice were injected intraperitoneally with BrdU (5-bromo-2-deoxy-uridine, Roche) labeling reagent at gestational day 12 or 13, with a dosage of 15 μl/g body weight. One hour after injection, embryos were dissected, fixed in Carnoy's fixative, dehydrated through graded ethanol, embedded in paraffin wax and sectioned at 5 μm thickness. Sections from anterior,

middle or posterior regions of the developing palatal shelves were selected for detection of BrdU-labeled cells by using the BrdU labeling and detection kit (Roche) following the manufacturer's protocol. Following BrdU detection, sections were counterstained with nuclear fast red (Vector Laboratories, Inc.) to label all cellular nuclei. The total number of cells and the number of BrdU-positive cells in the palatal epithelium and mesenchyme on each of five consecutive sections were counted. Cell proliferation index was calculated as the percentage of the total cells being BrdU-positive. ANOVA was applied for statistical analyses and a P value less than 0.01 was considered statistically significant.

For detection of Ki67, Paraffin sections from selected palatal regions of staged mouse embryos were stained with an antibody against Ki67 as described previously (Casey et al., 2006). Cell apoptosis was detected by TUNEL assays. Paraffin sections from selected palatal regions of staged mouse embryos were analyzed by using the DeadEnd™ Fluorometric TUNEL System (Promega) following the manufacturer's instructions.

Expression vectors and promoter-luciferase constructs

The *Mn1* expression vector was constructed by subcloning an *Mn1* cDNA fragment containing the full-length protein-coding region into the pcDNA3TOPO (Invitrogen) expression vector. The human *TBX22* promoter-luciferase reporter vectors (*pGL3-TBX22 hP0* and *pGL3-TBX22 hP1*) were described previously (Andreou et al., 2007). The mouse *Tbx22* promoter-luciferase reporter vectors were similarly constructed by PCR amplifying the mouse *Tbx22* promoter regions (Fig. S3) followed by subcloning into the pGL3-basic vector (Promega). All subcloned fragments were sequence verified.

Cell culture, transfection, and luciferase reporter assays

NIH3T3 cells were cultured in Dulbecco's modified Eagle's medium (DMEM) supplemented with 10% fetal bovine serum and 1% penicillin/streptomycin. For luciferase reporter assays, cells were plated in 24-well tissue culture plates (Corning) and co-transfected with 0.05 μg of a luciferase reporter vector, 0.05 μg of the pRL-Renilla luciferase expression vector (Promega), and increasing amounts of the *Mn1* expression vector. Transfections were performed by using the Lipofectamine reagents (Invitrogen) in accordance with the manufacture's instructions. Cells were cultured for 48 hours after transfection and then assayed using the Dual-Luciferase Assay Kit (Promega). Firefly luciferase activity was normalized to Renilla luciferase activity. All transfection experiments were carried out in triplicates and data were summarized from three repeat experiments.

Real-time RT-PCR

For detection of the effects of Mn1 on endogenous *Tbx22* gene expression, NIH3T3 cells were plated in 6-well tissue culture plates and transfected with increasing amounts of the *Mn1* expression vector. Cells were cultured for 48 hours after transfection and total RNA was extracted using Trizol reagents (Invitrogen). First strand cDNA was synthesized using SuperScript First-Strand Synthesis System (Invitrogen). Quantitative PCR amplifications were performed in an iCycler real-time PCR machine (Bio-Rad) using the SYBR GreenER™ qPCR Supermix (Invitrogen). *Mn1* gene-specific PCR primers are 5′-AGATCCAGCTGCAGAGACAA-3′ and 5′-TACTCATGGCGCTCTTGACT-3′. *Tbx22* gene-specific PCR primers are 5′-GACCTGTCCCTGATTGAGTCC-3′ and 5′-GCTGGTTTTGGTAAGCTGTCA-3′. *Hprt* gene-specific primers are 5'-TGCTGGTGAAAAGGACCTCTCG-3' and 5'-CTGGCAACATCAACAGGACTCC-3'. For each sample, the relative levels of *Mn1* and *Tbx22* mRNAs were normalized to that of HPRT using the standard curve method.

Results

Expression of *Mn1* mRNA during early mouse embryogenesis and in the developing palate

By whole mount in situ hybridization, *Mn1* mRNA expression was first detected at embryonic day E9.5 (Fig. 1A). At this stage, *Mn1* mRNA was strongly expressed in the midbrain and hindbrain tissues and in the craniofacial mesenchyme. By E10.5, *Mn1* mRNA was highly expressed in all of the prominences of the developing face, including frontonasal processes, maxillary processes, mandibular processes, and in the second branchial arch (Fig. 1, B and D). *Mn1* mRNA was also detected in a subset of mesenchymal cells in the developing somites and limb buds. This pattern of *Mn1* mRNA expression persists at E11.5 (Fig. 1, C and E). At this stage, palatal outgrowth had initiated on the oral sides of the maxillary processes and *Mn1* mRNA was strongly expressed in the palatal primordia (Fig. 1E). In situ hybridization of sections of E12.5 embryos showed that *Mn1* mRNA was highly expressed in the developing palatal mesenchyme and in the preossification mesenchymal cells in the mandible (Fig. 1F). Strong *Mn1* mRNA expression persists in the brain, in particular in the ventricular zone (Fig. 1F).

The reported cleft palate phenotype of the *Mn1* mutant mice prompted us to carry out a detailed analysis of *Mn1* mRNA expression during palate development. Recent studies have demonstrated that several genes exhibit differential expression along the anterior-posterior axis of the developing palatal shelves in mice (Zhang et al., 2002; Alappat et al., 2005; Yu et al., 2005; Hilliard et al., 2005; Li and Ding, 2007). The distinct gene expression patterns appear to divide the developing palatal shelves into three regions along the anterior-posterior axis: (1) anterior palate that expresses high levels of *Msx1* and *Shox2* mRNAs (Zhang et al., 2002; Hilliard et al., 2005; Yu et al., 2005); (2) middle palate (roughly corresponding to the region flanked by the upper first molar tooth germs, Alappat et al., 2005) that lacks *Msx1* expression and exhibits anterior-to-posterior expansion of *Shox2* mRNA expression from E12.5 to E14.5 (Li and Ding, 2007); and (3) posterior palate that expresses high levels of *Meox2* mRNA but lacks *Msx1* and *Shox2* mRNA expression (Li and Ding, 2007). In situ hybridization of serial sections of the developing palatal shelves showed that *Mn1* mRNA is differentially expressed along the anterior-posterior axis of the developing palatal shelves, with high levels of expression in both mesenchyme and epithelium in the middle and posterior regions and very low levels in the anterior region of the palatal shelves during the vertical growth period from E12.5 to E13.5 as well as after palatal shelf elevation at E14.5 (Fig. 2).

Mn1$^{-/-}$ mutant mice exhibit palatal retardation and failure of palatal shelf elevation

To investigate which palatal developmental steps require Mn1 function, we carried out detailed histological analyses of *Mn1*$^{-/-}$ mouse embryos throughout palate development. *Mn1*$^{-/-}$ mutant embryos displayed normal palatal shelf outgrowth at E12.5 (data not shown). At E13.5, the palatal shelves of *Mn1*$^{-/-}$ mutant embryos exhibited similar size and shape with those of wild-type embryos (Fig. 3A, B). By E14.5, the palatal shelves of wild-type embryos had already elevated to the horizontal position and initiated fusion by forming the midline epithelial seam (Fig. 3C), which was disintegrated by E15.5 to form the fused secondary palate (Fig. 3E). In contrast, the bilateral palatal shelves of *Mn1*$^{-/-}$ mutant embryos failed to elevate and remained at the vertical position at E14.5 and at E15.5 (Fig. 3, D and F).

Histological analyses of *Mn1*$^{-/-}$ mutant embryos at later stages revealed different fates of the palatal shelves along the anterior-posterior axis. At E16.5, the middle and posterior palatal shelves in *Mn1*$^{-/-}$ mutant embryos were still vertically oriented and appeared greatly reduced in size (Fig. 4B). By E18.5, the posterior palatal shelves were further retarded and retracted to the maxillary processes (Fig. 4D), while the anterior palatal shelves were still clearly visible and often elevated on one or both sides (Fig. 4C).

Mn1 is required for proper palatal shelf growth

Impairment of palatal shelf elevation is often accompanied by and partially due to retarded palatal shelf growth, as has been reported in the *Osr2*$^{-/-}$ mutant mice (Lan et al., 2004). To investigate the cellular mechanisms of palatal shelf retardation and elevation failure in *Mn1*$^{-/-}$ mutant mice, we examined whether there are alterations in cell proliferation and cell survival during palate development in *Mn1*$^{-/-}$ mutant mice. No differences in cell apoptosis were found in the palatal shelves between wild-type and *Mn1*$^{-/-}$ mutant embryos at E12.5 and at E13.5 (data not shown). No significant alterations in cell proliferation were observed in the palatal shelves in *Mn1*$^{-/-}$ mutant embryos at E12.5 (data not shown). At E13.5, we detected a 57% reduction ($P<0.01$) in the posterior and a 49% reduction ($P<0.01$) in the middle regions of the palatal mesenchyme in *Mn1*$^{-/-}$ mutant embryos in comparison with their wild-type littermates (Fig. 5G). In contrast, the cell proliferation index was not significantly different in the anterior palatal mesenchyme in the same *Mn1*$^{-/-}$ mutant and wild-type embryos (Fig 5G). Similarly, palatal epithelial cell proliferation was also significantly reduced in the middle and posterior palate but not in the anterior palate in *Mn1*$^{-/-}$ mutant embryos, in comparison with the wild-type littermates (Fig. 5H). The selective reduction in palatal cell proliferation in the middle and posterior regions of the palatal shelves in *Mn1*$^{-/-}$ mutant mice correlates with the differential expression of *Mn1* mRNA along the anterior-posterior axis during normal palate development.

To understand the dramatic retardation of the palatal shelves at later stages in *Mn1*$^{-/-}$ mutant embryos, we also examined cell proliferation and cell apoptosis in E14.5 and E15.5 embryos. The decrease in cell proliferation rate in the posterior and middle regions of the palatal shelves in the *Mn1*$^{-/-}$ mutant embryos continued through E15.5 (Fig. 6 A-C and data not shown), indicating that Mn1 is an important regulator of palatal shelf growth before and after palatal shelf elevation. Moreover, by TUNEL assays, we detected increased apoptosis at E15.5 in the posterior regions of the palatal mesenchyme in *Mn1*$^{-/-}$ mutant embryos (Fig. 6D, E). These data indicate that the dramatic degeneration of the posterior palatal shelves observed by E18.5 in *Mn1*$^{-/-}$ mutant embryos resulted from decreased proliferation and increased apoptosis in the posterior palatal shelves, in combination with retraction of the freely projecting palatal shelves into the maxillary processes due to the morphogenetic expansion of the craniofacial width.

Palatal shelf growth defect in *Mn1*$^{-/-}$ mutants is accompanied by a region-specific decrease in *CyclinD2* expression

Several molecular pathways have been shown to regulate cell proliferation during palate development by regulating the expression of D-type cyclins. D-type cyclins are important cell cycle regulators, which bind CDK4 or CDK6 to control cell cycle progression through the G1 phase (Matsushime et al., 1991; Xiong et al., 1991; Motokura et al., 1991; Morgan et al., 1997). Conditional inactivation of *Tgfβr2* in cranial neural crest (CNC) cells down-regulated CyclinD1 expression and reduced CNC cell proliferation in the palatal mesenchyme (Ito et al., 2003). Msx1 regulates neural crest cell proliferation and differentiation also through maintaining CyclinD1 expression (Hu et al., 2001). To understand the cellular mechanism by which Mn1 regulates palatal growth in the middle and posterior palatal shelves, we investigated possible alterations in the expression levels of D-type cyclins in *Mn1*$^{-/-}$ mutant embryos. No change in the levels of *CyclinD1* expression was detected in either the epithelium or mesenchyme of the developing palate in *Mn1*$^{-/-}$ embryos in comparison with wild-type littermates (data not shown). In contrast, the expression of *CyclinD2* is reduced in the middle and posterior regions of the palatal mesenchyme as well as in the posterior palatal epithelium in *Mn1*$^{-/-}$ embryos at E13.5 (Fig. 7). These data suggest that Mn1 regulates palatal shelf growth, at least in part, through maintaining *CyclinD2* expression in the middle and posterior palatal shelves.

Effects of *Mn1* deficiency on palatal gene expression

To investigate the molecular mechanisms involving Mn1 in palate development, we examined the expression patterns of other genes known to play important role in palate development, including *Fgf10*, *Fgfr2*, *Osr2*, *Shh*, *Patch1*, *Pax9*, *Shox2*, and *Tgfβ3*. No obvious differences in either levels or patterns of expression of these genes were found in the developing palatal shelves in wild-type and *Mn1*$^{-/-}$ mutant embryos (Fig. 8 and Supplemental Fig. 1). In particular, the differential expression patterns of *Fgf10*, *Shox2*, and *Meox2* mRNAs along the anterior-posterior axis of the developing palatal shelves are maintained in the *Mn1*$^{-/-}$ mutant embryos (Fig. 8), indicating that there is no gross anterior-posterior patterning defects in the developing palate in *Mn1*$^{-/-}$ mutant embryos.

Extensive expression analyses of other genes implicated in palate development showed that expression of *Tbx22*, homologous to the gene associated with CPX in humans, is specifically reduced in the developing palatal shelves in *Mn1*$^{-/-}$ mutant embryos (Fig. 9). Interestingly, expression of *Tbx22* mRNA also exhibits a posterior preference in the developing palatal shelves, similar to the expression pattern of *Mn1*, during normal palate development in mice (Fig. 9A-C). Compared to wild-type embryos, the expression levels of *Tbx22* are dramatically reduced in the middle and posterior palatal shelves of *Mn1*$^{-/-}$ mutant embryos (Fig. 9D-F), indicating that Mn1 and Tbx22 function in the same molecular pathway to regulate mammalian palate development.

Mn1 is a transcriptional activator of *Tbx22* gene expression

The similar expression patterns of *Mn1* and *Tbx22* mRNAs in the developing wild-type palatal shelves and the specific down-regulation of *Tbx22* mRNA in *Mn1*$^{-/-}$ mutant embryos suggest that Mn1 may directly regulate *Tbx22* gene expression during palate development. We previously showed that the human *TBX22* gene is transcribed from two different promoters that are approximately 10 Kb apart (Andreou et al., 2007). Quantitative RT-PCR assays of human embryonic RNA samples indicated that embryonic *TBX22* mRNA expression was predominantly generated by the *hP0* promoter (data not shown). Analyses of 5' RACE (rapid amplification of cDNA ends) products from E12.5 mouse embryonic craniofacial RNA templates revealed that the mouse *Tbx22* gene is also transcribed from at least two distinct promoters, a distal promoter corresponding to the human *TBX22 hP0* and a proximal promoter corresponding to the human *TBX22 hP1* (Fig. S2). Interestingly, the previously determined core binding DNA sequence for the Mn1 transcription factor, CACCC, is present in various locations within 2 Kb of the transcription start site for each of the mouse and human *TBX22* promoters (Figure S3). To investigate whether Mn1 can activate transcription from the mouse and human *TBX22* gene promoters, we constructed *Tbx22* promoter-luciferase reporter plasmids (see Materials and Methods) and tested the effects of *Mn1* co-transfection on luciferase reporter expression in NIH3T3 cells. Transfection of each of the promoter-luciferase plasmids showed that the mouse *mP0* and *mP1* as well as human *hP0* promoters each had promoter activity in NIH3T3 cells, with the *hP0* promoter being three-fold stronger than the *mP0* or *mP1* promoter (Fig. 10A). In contrast, the *hP1*-luciferase construct did not show promoter activity in NIH3T3 and three other cell lines tested (Fig. 10A) (Andreou et al., 2007, and data not shown). Co-transfection with the *Mn1* expression vector resulted in a dose-dependent increase in luciferase expression from each of the *mP0*-, *mP1*-, and *hP0*-luciferase constructs but not the *hP1* promoter-luciferase construct (Fig. 10A). Moreover, transfection of NIH3T3 cells with the *Mn1* expression vector resulted in a dose-dependent increase in endogenous *Tbx22* mRNA expression (Fig. 10B,C). These data indicate that Mn1 functions as a transcriptional activator of *Tbx22* gene expression.

Discussion

Cleft palate is a common birth defect in humans, occurring in approximately 1 in 1000 live births (Vanderas, 1987; Schutte and Murray, 1999; Gorlin et al., 2001). Approximately 50% of cleft palate cases are non-syndromic, although cleft palate has been associated with more than 300 syndromic developmental disorders. Several genes underlying syndromic forms of cleft palate have been identified, including *IRF6* (Van der Woude and popliteal pterygium syndromes) (Kondo et al., 2002), *MSX1* (cleft lip or palate with hypodontia) (van den Boogaard et al., 2000), *P63* (ectodermal dysplasia and cleft lip or palate) (Celli et al., 1999; Ianakiev et al., 2000), *PVRL1* (autosomal recessive cleft lip/palate with ectodermal dysplasia) (Suzuki et al., 2000), and *TBX22* (CPX) (Braybrook et al., 2001). In addition, genetic studies in mice have revealed that mutations in more than sixty different genes each resulted in cleft palate and have uncovered specific molecular and cellular mechanisms controlling palate development (reviewed by Gritli-Linde, 2007). Interestingly, recent studies have demonstrated that palatal shelf growth is differentially regulated along the anterior-posterior axis (reviewed by Hilliard et al., 2005). Zhang et al. (2002) first demonstrated that *Msx1* and *Bmp4* are both only expressed in and required for the growth of the anterior region of the developing palatal shelves. In palatal explant culture assays, exogenous Bmp4 induced *Msx1* mRNA expression and increased cell proliferation in the anterior but not in posterior palatal mesenchyme (Zhang et al., 2002; Hilliard et al., 2005). The Shox2 transcription factor is also specifically expressed in the anterior palate and mice lacking *Shox2* exhibited growth defects in the anterior but not posterior regions of the developing palatal shelves (Yu et al., 2005). However, previous studies have also showed that the anterior and posterior palatal regions have similar cell proliferation rates during palatal outgrowth (Zhang et al., 2002; Li and Ding, 2007), suggesting that there must be factors that preferentially regulate posterior palatal growth. Our finding that Mn1 is differentially expressed along the anterior-posterior axis and preferentially regulates middle and posterior palatal cell proliferation fills a longstanding gap in the understanding of the molecular mechanisms of palate development.

Mn1 specifically regulates *Tbx22* gene expression during palate development

Mutations in the human *TBX22* gene, including nonsense, frameshift, splice-site and missense changes, have been associated with CPX (Braybrook et al., 2001;2002;Chaabouni et al., 2005). In addition, mutation-screening studies of patients with isolated cleft palate showed that mutations in *TBX22* represent the most common single cause of cleft palate known (Marcano et al., 2004;Suphapeetiporn et al., 2007). These data suggest that TBX22 plays primary and critical roles in palate development. Consistent with this hypothesis, Braybrook et al. (2002) showed that *TBX22* mRNA is strongly expressed in the developing human palatal shelves prior to palatal elevation and fusion. *TBX22* mRNA expression was also detected in the base of the developing tongue, which correlated well with the ankyloglossia phenotype in CPX patients. Several laboratories independently isolated the mouse *Tbx22* gene and reported *Tbx22* mRNA expression in the developing palatal shelves and at the base of the developing tongue (Braybrook et al., 2002;Bush et al., 2002;Herr et al., 2003). Although the exact roles of *Tbx22* in palate development remain to be elucidated, these studies showed that palatal expression of *Tbx22* mRNA was high during vertical palatal growth and declined after palatal shelf elevation in both human and mice, suggesting that Tbx22 may play a conserved role in palatal shelf growth. Welsh et al. (2007) showed, by whole mount in situ hybridization, that *Tbx22* mRNA is preferentially expressed in the posterior palate in E13.5 and E14.5 mouse embryos. We confirmed, by using section in situ hybridization, the differential expression of *Tbx22* mRNA along the anterior-posterior axis of the developing secondary palate (Fig. 9). Interestingly, *Tbx22* mRNA expression was dramatically down-regulated in the $Mn1^{-/-}$ mutant palatal shelves. The fact that palatal expression of many genes, including that of *Meox2*, which is also preferentially expressed in the posterior palate during palatal outgrowth (Li and Ding,

2007, and Fig. 8), is not affected by *Mn1* deficiency indicates that *Tbx22* is a specific downstream target of Mn1. Our data that Mn1 activated, in a dose-dependent manner, expression of endogenous *Tbx22* mRNA and the luciferase reporter gene driven by either the human or mouse *Tbx22* promoter sequences in transfected NIH3T3 cells provide further support that Mn1 activates transcription of the *Tbx22* gene. These data link two spatially co-expressed transcription factors in a novel molecular pathway for the regulation of posterior palate development.

Primary and secondary effects of *Mn1* deficiency on palate development

It was previously suggested that the cleft palate defect in the $Mn1^{-/-}$ mutant mice might be secondary to the severe cranial skeletal defects (Meester-Smoor et al., 2005). We found that Mn1 is differentially expressed along the anterior-posterior axis of the developing palatal shelves and required for proper palatal growth in the middle and posterior regions but not in the anterior region. The specific down-regulation of *Tbx22* mRNA expression in the $Mn1^{-/-}$ mutant palatal shelves also identifies a primary role for Mn1 in palate development. However, $Mn1^{-/-}$ mutant mice exhibit complete cleft of the secondary palate, although no significant growth deficiency was found in the anterior palate at any stage of palate development. In addition, the palatal shelves failed to elevate, in particular in the middle and posterior regions, in the $Mn1^{-/-}$ mutant mice. Impairment of palatal shelf elevation is often caused by mechanical hindrance, such as aberrant palatal-tongue and palatal-mandible fusions in the $Jag2^{-/-}$ and $Fgf10^{-/-}$ mutant mice, respectively (Casey et al., 2006; Alappat et al., 2005). Defects in mandibular development or deformation of the tongue have also been suggested as causes of failure of palatal shelf elevation in several mutant mouse strains, including $Ryk^{-/-}$ and $Foxf2^{-/-}$ mutant mice (Halford et al., 2000; Wang et al., 2003). In addition, $Pax9^{-/-}$ mutant mice exhibited impairment of palatal shelf elevation attributable to deformation of the palatal shelves themselves (Peters et al., 1998). $Mn1^{-/-}$ mutant mice exhibited normal mandibular development (Meester-Smoor et al., 2005). However, the developing tongue did not properly descend to the floor of the mouth during the time of palatal shelf elevation in the $Mn1^{-/-}$ mutant mice, in comparison with that in the wild-type littermates (Fig. 3). Whereas *Mn1* mRNA is strongly expressed in the middle and posterior palatal mesenchyme, little *Mn1* expression was observed in the developing tongue (Fig. 2). Thus, the palatal elevation defect in the $Mn1^{-/-}$ mutant mice may be due to an intrinsic defect in the palatal shelves or secondary to as yet unidentified defects in a mandibular component involved in tongue movement. Taken together, the cleft palate phenotype in $Mn1^{-/-}$ mutant mice likely results from a combination of the primary defects in palatal growth and secondary effects of other craniofacial abnormalities.

Supplementary Material

Refer to Web version on PubMed Central for supplementary material.

Acknowledgement

This work was supported by the NIH/NIDCR grants R01DE013681 and R01DE015207 to RJ.

References

Alappat SR, Zhang Z, Suzuki K, Zhang X, Liu H, Jiang R, Yamada G, Chen Y. The cellular and molecular etiology of the cleft secondary palate in *Fgf10* mutant mice. Dev. Biol 2005;277:102–113. [PubMed: 15572143]

Andreou AM, Pauws E, Jones MC, Singh MK, Bussen M, Doudney K, Moore GE, Kispert A, Brosens JJ, Stanier P. *TBX22* missense mutations found in patients with X-linked cleft palate affect DNA binding, sumoylation, and transcriptional repression. Am. J. Hum. Genet 2007;81:700–712. [PubMed: 17846996]

Braybrook C, Doudney K, Marçano AC, Arnason A, Bjornsson A, Patton MA, Goodfellow PJ, Moore GE, Stanier P. The T-box transcription factor gene *TBX22* is mutated in X-linked cleft palate and ankyloglossia. Nat. Genet 2001;29:179–183. [PubMed: 11559848]

Braybrook C, Lisgo S, Doudney K, Henderson D, Marçano AC, Strachan T, Patton MA, Villard L, Moore GE, Stanier P, Lindsay S. Craniofacial expression of human and murine *TBX22* correlates with the cleft palate and ankyloglossia phenotype observed in CPX patients. Hum. Mol. Genet 2002;11:2793–804. [PubMed: 12374769]

Buijs A, Sherr S, van Baal S, van Bezouw S, van der Plas D, van Kessel A. Geurts, Riegman P, Deprez R. Lekanne, Zwarthoff E, Hagemeijer A. Translocation (12;22) (p13;q11) in myeloproliferative disorders results in fusion of the ETS-like *TEL* gene on 12p13 to the MN1 gene on 22q11. Oncogene 1995;10:1511–1519. [PubMed: 7731705]

Buijs A, van Rompaey L, Molijn AC, Davis JN, Vertegaal AC, Potter MD, Adams C, van Baal S, Zwarthoff EC, Roussel MF, Grosveld GC. The MN1-TEL fusion protein., encoded by the translocation (12;22)(p13;q11) in myeloid leukemia, is a transcription factor with transforming activity. Mol. Cell. Biol 2000;20:9281–93. [PubMed: 11094079]

Bush JO, Lan Y, Maltby KM, Jiang R. Isolation and developmental expression analysis of *Tbx22*, the mouse homolog of the human X-linked cleft palate gene. Dev. Dyn 2002;225:322–6. [PubMed: 12412015]

Carella C, Bonten J, Rehg J, Grosveld GC. MN1-TEL, the product of the t(12;22) in human myeloid leukemia, immortalizes murine myeloid cells and causes myeloid malignancy in mice. Leukemia 2006;20:1582–92. [PubMed: 16810199]

Carella C, Bonten J, Sirma S, Kranenburg TA, Terranova S, Klein-Geltink R, Shurtleff S, Downing JR, Zwarthoff EC, Liu PP, Grosveld GC. *MN1* overexpression is an important step in the development of inv(16) AML. Leukemia 2007;21:1679–90. [PubMed: 17525718]

Casey LM, Lan Y, Cho ES, Maltby KM, Gridley T, Jiang R. Jag2-Notch1 signaling regulates oral epithelial differentiation and palate development. Dev. Dyn 2006;235:1830–44. [PubMed: 16607638]

Celli J, Duijf P, Hamel BC, Bamshad M, Kramer B, Smits AP, Newbury-Ecob R, Hennekam RC, Van Buggenhout G, van Haeringen A, Woods CG, van Essen AJ, de Waal R, Vriend G, Haber DA, Yang A, McKeon F, Brunner HG, van Bokhoven H. Heterozygous germline mutations in the *p53* homolog *p63* are the cause of EEC syndrome. Cell 1999;99:143–53. [PubMed: 10535733]

Chai Y, Maxson RE Jr. Recent advances in craniofacial morphogenesis. Dev. Dyn 2006;235:2353–75. [PubMed: 16680722]

Chaabouni M, Smaoui N, Benneji N, M'rd R, Jemaa LB, Hachicha S, Chaabouni H. Mutation analysis of *TBX22* reveals new mutation in Tunisian CPX family. Clin. Dysmorphol 2005;14:23–25. [PubMed: 15602089]

Du Y, Jenkins NA, Copeland NG. Insertional mutagenesis identifies genes that promote the immortalization of primary bone marrow progenitor cells. Blood 2005;106:3932–9. [PubMed: 16109773]

Ferguson MW. Palate development. Development Suppl 1988;103:41–60.

Grosveld GC. MN1, a novel player in human AML. Blood. Cells. Mol. Dis 2007;39:336–9. [PubMed: 17698380]

Gorlin, RJ.; Cohen, MM., Jr.; Hennekam, RCM. Oxford University Press; New York: 2001. Syndromes of the head and neck.

Gritli-Linde A. Molecular control of secondary palate development. Dev. Biol 2007;301:309–26. [PubMed: 16942766]

Halford MM, Armes J, Buchert M, Meskenaite V, Grail D, Hibbs ML, Wilks AF, Farlie PG, Newgreen DF, Hovens CM, Stacker SA. *Ryk*-deficient mice exhibit craniofacial defects associated with perturbed Eph receptor crosstalk. Nat. Genet 2000;25:414–418. [PubMed: 10932185]

Han J, Ito Y, Yeo JY, Sucov HM, Maas R, Chai Y. Cranial neural crest-derived mesenchymal proliferation is regulated by Msx1-mediated p19(INK4d) expression during odontogenesis. Dev. Biol 2003;261:183–196. [PubMed: 12941628]

Herr A, Meunier D, Müller I, Rump A, Fundele R, Ropers HH, Nuber UA. Expression of mouse *Tbx22* supports its role in palatogenesis and glossogenesis. Dev. Dyn 2003;226:579–586. [PubMed: 12666195]

Heuser M, Beutel G, Krauter J, Döhner K, von Neuhoff N, Schlegelberger B, Ganser A. High meningioma 1 (MN1) expression as a predictor for poor outcome in acute myeloid leukemia with normal cytogenetics. Blood 2006;108:3898–905. [PubMed: 16912223]

Hilliard SA, Yu L, Gu S, Zhang Z, Chen YP. Regional regulation of palatal growth and patterning along the anterior-posterior axis in mice. J. Anat 2005;207:655–667. [PubMed: 16313398]

Hu G, Lee H, Price SM, Shen MM, Abate-Shen C. *Msx* homeobox genes inhibit differentiation through upregulation of cyclin D1. Development 2001;128:2373–2384. [PubMed: 11493556]

Ianakiev P, Kilpatrick MW, Toudjarska I, Basel D, Beighton P, Tsipouras P. Split-hand/split-foot malformation is caused by mutations in the p63 gene on 3q27. Am. J. Hum. Genet 2000;67:59–66. [PubMed: 10839977]

Ito Y, Yeo JY, Chytil A, Han J, Bringas P Jr. Nakajima A, Shuler CF, Moses HL, Chai Y. Conditional inactivation of *Tgfbr2* in cranial neural crest causes cleft palate and calvaria defects. Development 2003;130:5269–5280. [PubMed: 12975342]

Jin JZ, Ding J. Analysis of *Meox2* mutant mice reveals a novel postfusion-based cleft palate. Dev. Dyn 2006;235:539–546. [PubMed: 16284941]

Kawagoe H, Grosveld GC. Conditional *MN1-TEL* knock-in mice develop acute myeloid leukemia in conjunction with overexpression of *HOXA9*. Blood 2005a;106:4269–77. [PubMed: 16105979]

Kawagoe H, Grosveld GC. MN1-TEL myeloid oncoprotein expressed in multipotent progenitors perturbs both myeloid and lymphoid growth and causes T-lymphoid tumors in mice. Blood 2005b;106:4278–86. [PubMed: 16081688]

Kondo S, Schutte BC, Richardson RJ, Bjork BC, Knight AS, Watanabe Y, Howard E, de Lima RL, Daack-Hirsch S, Sander A, McDonald-McGinn DM, Zackai EH, Lammer EJ, Aylsworth AS, Ardinger HH, Lidral AC, Pober BR, Moreno L, Arcos-Burgos M, Valencia C, Houdayer C, Bahuau M, Moretti-Ferreira D, Richieri-Costa A, Dixon MJ, Murray JC. Mutations in *IRF6* cause Van der Woude and popliteal pterygium syndromes. Nat Genet 2002;32:285–9. [PubMed: 12219090]

Lan Y, Kingsley PD, Cho ES, Jiang R. *Osr2*, a new mouse gene related to Drosophila odd-skipped, exhibits dynamic expression patterns during craniofacial, limb, and kidney development. Mech. Dev 2001;107:175–179. [PubMed: 11520675]

Lan Y, Ovitt CE, Cho ES, Maltby KM, Wang Q, Jiang R. *Odd-skipped related 2* (*Osr2*) encodes a key intrinsic regulator of secondary palate growth and morphogenesis. Development 2004;131:3207–3216. [PubMed: 15175245]

Deprez, R. H. Lekanne; Riegman, PH.; Groen, NA.; Warringa, UL.; van Biezen, NA.; Molijn, AC.; Bootsma, D.; de Jong, PJ.; Menon, AG.; Kley, NA., et al. Cloning and characterization of *MN1*, a gene from chromosome 22q11, which is disrupted by a balanced translocation in a meningioma. Oncogene 1995;10:1521–1528. [PubMed: 7731706]

Li Q, Ding J. Gene expression analysis reveals that formation of the mouse anterior secondary palate involves recruitment of cells from the posterior side. Int. J. Dev. Biol 2007;51:167–172. [PubMed: 17294368]

Liu W, Sun X, Braut A, Mishina Y, Behringer RR, Mina M, Martin JF. Distinct functions for Bmp signaling in lip and palate fusion in mice. Development 2005;132:1453–61. [PubMed: 15716346]

Marcano ACB, Doudney K, Braybrook C, Squires R, Patton MA, Lees M, Richieri-Costa A, Lidral AC, Murray JC, Moore GE, et al. *TBX22* mutations are a frequent cause of cleft palate. J. Med. Genet 2004;41:68–74. [PubMed: 14729838]

Matsushime H, Roussel MF, Ashmun RA, Sherr CJ. Colony-stimulating factor 1 regulates novel cyclins during the G1 phase of the cell cycle. Cell 1991;65:701–713. [PubMed: 1827757]

Meester-Smoor MA, Molijn AC, Zhao Y, Groen NA, Groffen CA, Boogaard M, van Dalsum-Verbiest D, Grosveld GC, Zwarthoff EC. The MN1 oncoprotein activates transcription of the *IGFBP5* promoter through a CACCC-rich consensus sequence. J. Mol. Endocrinol 2007;38:113–25. [PubMed: 17242174]

Meester-Smoor MA, Vermeij M, van Helmond MJ, Molijn AC, van Wely KH, Hekman AC, Vermey-Keers C, Riegman PH, Zwarthoff EC. Targeted disruption of the *Mn1* oncogene results in severe

defects in development of membranous bones of the cranial skeleton. Mol. Cell. Biol 2005;25:4229–4236. [PubMed: 15870292]

Morgan DO. Cyclin-dependent kinases: engines, clocks, and microprocessors. Annu. Rev. Cell. Dev. Biol 1997;13:261–291. [PubMed: 9442875]

Motokura T, Bloom T, Kim HG, Jüppner H, Ruderman JV, Kronenberg HM, Arnold A. A novel cyclin encoded by a *bcl1*-linked candidate oncogene. Nature 1991;350:512–515. [PubMed: 1826542]

Peters H, Neubüser A, Kratochwil K, Balling R. *Pax9*-deficient mice lack pharyngeal pouch derivatives and teeth and exhibit craniofacial and limb abnormalities. Genes. Dev 1998;12:2735–2747. [PubMed: 9732271]

Rice R, Spencer-Dene B, Connor EC, Gritli-Linde A, McMahon AP, Dickson C, Thesleff I, Rice DPC. Disruption of Fgf10/Fgfr2b-coordinated epithelial-mesenchymal interactions causes cleft palate. J. Clin. Invest 2004;113:1692–1700. [PubMed: 15199404]

Ross ME, Mahfouz R, Onciu M, Liu HC, Zhou X, Song G, Shurtleff SA, Pounds S, Cheng C, Ma J, Ribeiro RC, Rubnitz JE, Girtman K, Williams WK, Raimondi SC, Liang DC, Shih LY, Pui CH, Downing JR. Gene expression profiling of pediatric acute myelogenous leukemia. Blood 2004;104:3679–87. [PubMed: 15226186]

Schutte BC, Murray JC. The many faces and factors of orofacial clefts. Hum. Mol. Genet 1999;8:1853–1859. [PubMed: 10469837]

Sperber, GH. Palatogenesis: closure of the secondary palate. In: Wyszynski, DF., editor. Cleft Lip & Palate, From Origin To Treatment. Oxford University Press; 2002. p. 14-24.

Suphapeetiporn K, Tongkobpetch S, Siriwan P, Shotelersuk V. TBX22 mutations are a frequent cause of non-syndromic cleft palate in the Thai population. Clin. Genet 2007;72:478–483. [PubMed: 17868388]

Sutton AL, Zhang X, Ellison TI, Macdonald PN. The 1,25(OH)2D3-regulated transcription factor MN1 stimulates vitamin D receptor-mediated transcription and inhibits osteoblastic cell proliferation. Mol. Endocrinol 2005;19:2234–44. [PubMed: 15890672]

Suzuki K, Hu D, Bustos T, Zlotogora J, Richieri-Costa A, Helm s J. A. Spritz RA. Mutations of *PVRL1*, encoding a cell-cell adhesion molecule/herpesvirus receptor, in cleft lip/palate-ectodermal dysplasia. Nat. Genet 2000;25:427–30. [PubMed: 10932188]

Valk PJ, Delwel R, Löwenberg B. Gene expression profiling in acute myeloid leukemia. Curr. Opin. Hematol 2004;12:76–81. [PubMed: 15604895]

van den Boogaard MJ, Dorland M, Beemer FA, van Amstel HK. *MSX1* mutation is associated with orofacial clefting and tooth agenesis in humans. Nat. Genet 2000;24:342–3. [PubMed: 10742093]

van Wely KH, Molijn AC, Buijs A, Meester-Smoor MA, Aarnoudse AJ, Hellemons A, den Besten P, Grosveld GC, Zwarthoff EC. The MN1 oncoprotein synergizes with coactivators RAC3 and p300 in RAR-RXR-mediated transcription. Oncogene 2003;22:699–709. [PubMed: 12569362]

Vanderas AP. Incidence of cleft lip, cleft palate, and cleft lip and palate among races: a review. Cleft. Palate. J 1987;24:216–225. [PubMed: 3308178]

Wang T, Tamakoshi T, Uezato T, Shu F, Kanzaki-Kato N, Fu Y, Koseki H, Yoshida N, Sugiyama T, Miura N. Forkhead transcription factor Foxf2 (LUN)-deficient mice exhibit abnormal development of secondary palate. Dev. Biol 2003;259:83–94. [PubMed: 12812790]

Welsh IC, Hagge-Greenberg A, O'Brien TP. A dosage-dependent role for Spry2 in growth and patterning during palate development. Mech. Dev 2007;124:746–761. [PubMed: 17693063]

Xiong Y, Connolly T, Futcher B, Beach D. Human D-type cyclin. Cell 1991;65:691–699. [PubMed: 1827756]

Yu L, Gu S, Alappat S, Song Y, Yan M, Zhang X, Zhang G, Jiang Y, Zhang Z, Zhang Y, Chen Y. *Shox2*-deficient mice exhibit a rare type of incomplete clefting of the secondary palate. Development 2005;132:4397–4406. [PubMed: 16141225]

Zhang Y, Zhao X, Hu Y, ***St Amand T, Zhang M, Ramamurthy R, Qiu M, Chen Y. *Msx1* is required for the induction of Patched by Sonic hedgehog in the mammalian tooth germ. Dev. Dyn 1999;215:45–53. [PubMed: 10340755]

Zhang Z, Song Y, Zhao X, Zhang X, Fermin C, Chen Y. Rescue of cleft palate in *Msx1*-deficient mice by transgenic Bmp4 reveals a network of BMP and Shh signaling in the regulation of mammalian palatogenesis. Development 2002;129:4135–4146. [PubMed: 12163415]

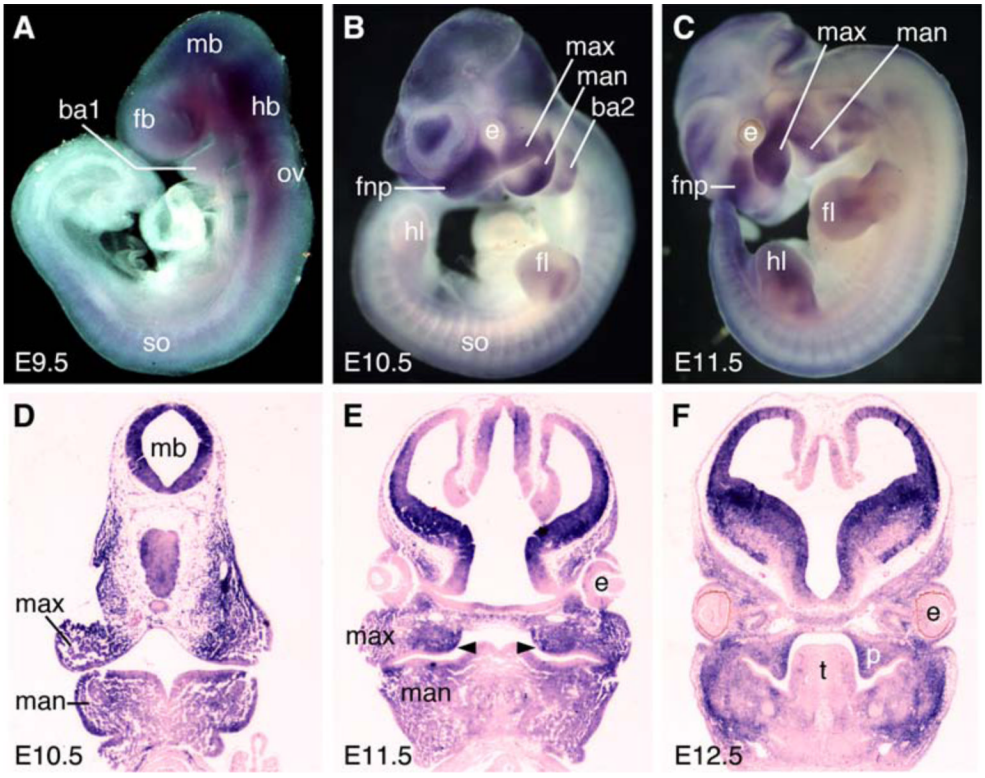

Fig. 1.

Expression pattern of *Mn1* mRNA in developing mouse embryos. mRNA signals were detected by whole mount in situ hybridization (A-C) or section in situ hybridization (D-F). (A) *Mn1* mRNA expression was first detected in the developing brain tissues and in the craniofacial mesenchyme at E9.5. (B-E) Strong *Mn1* mRNA expression was observed in the developing brain, frontonasal processes, maxillary processes, mandibular processes, the second branchial arch, the developing somites and limb buds at E10.5 (B, D) and E11.5 (C, E). (F) Section in situ hybridization showing strong *Mn1* mRNA expression in the developing palatal mesenchyme and in the preossification mesenchymal cells in the mandible. ba1, first branchial arch; ba2, second branchial arch; e, eye; fb, forebrain; fl, forelimb; fnp, frontonasal process; hb, hindbrain; hl, hindlimb; man, mandibular process; max, maxillary process; mb, midbrain; ov, otic vesicle; p, palatal shelf; so, somite; t, tongue.

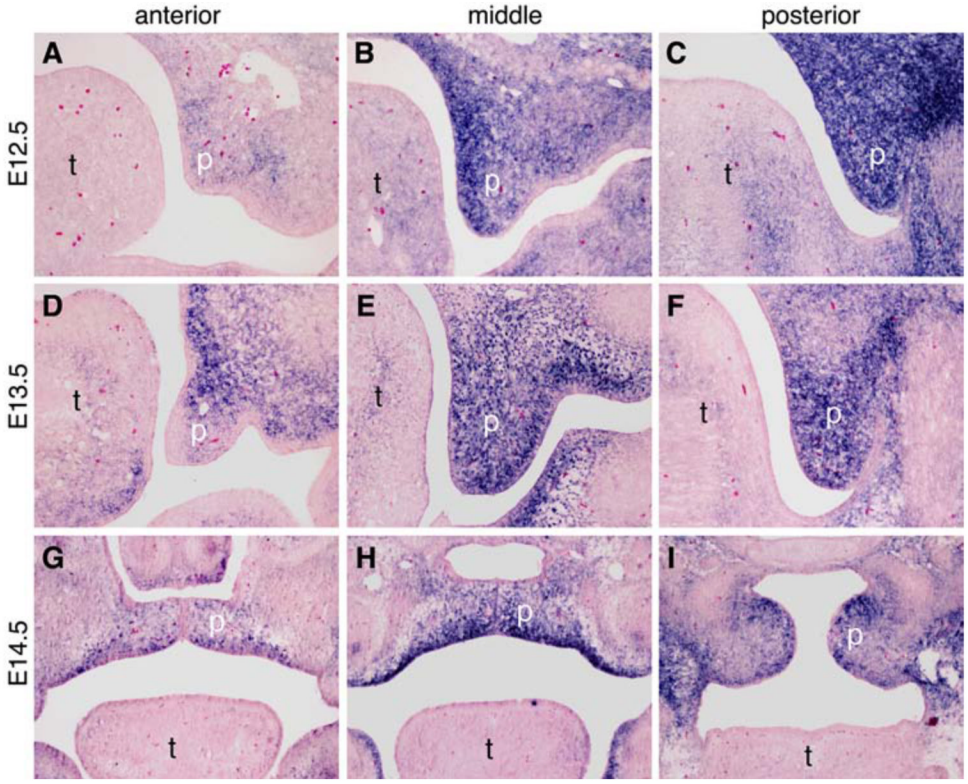

Fig. 2.

The expression pattern of *Mn1* mRNA along the anterior-posterior axis of the developing palate. Middle palate corresponds to the palatal region flanked by the maxillary first molar tooth germs. (A-C) At E12.5, *Mn1* mRNA expression in the developing secondary palate exhibits an anterior-posterior gradient, with low levels in the anterior palate (A), moderate levels in the middle palate (B), and highest levels in the posterior palate (C). (D-F) At E13.5, *Mn1* mRNA expression is still high in the middle (E) and posterior (F) regions and much weaker in the anterior region (D) of the developing palate. (G-I) At E14.5, the bilateral palatal shelves have elevated to the horizontal position above the tongue and have initiated contact and fusion in the anterior (G) and middle (H) regions. *Mn1* mRNA expression remains strong in the middle and posterior palatal regions and relatively weak in the anterior palate. p, palatal shelf; t, tongue.

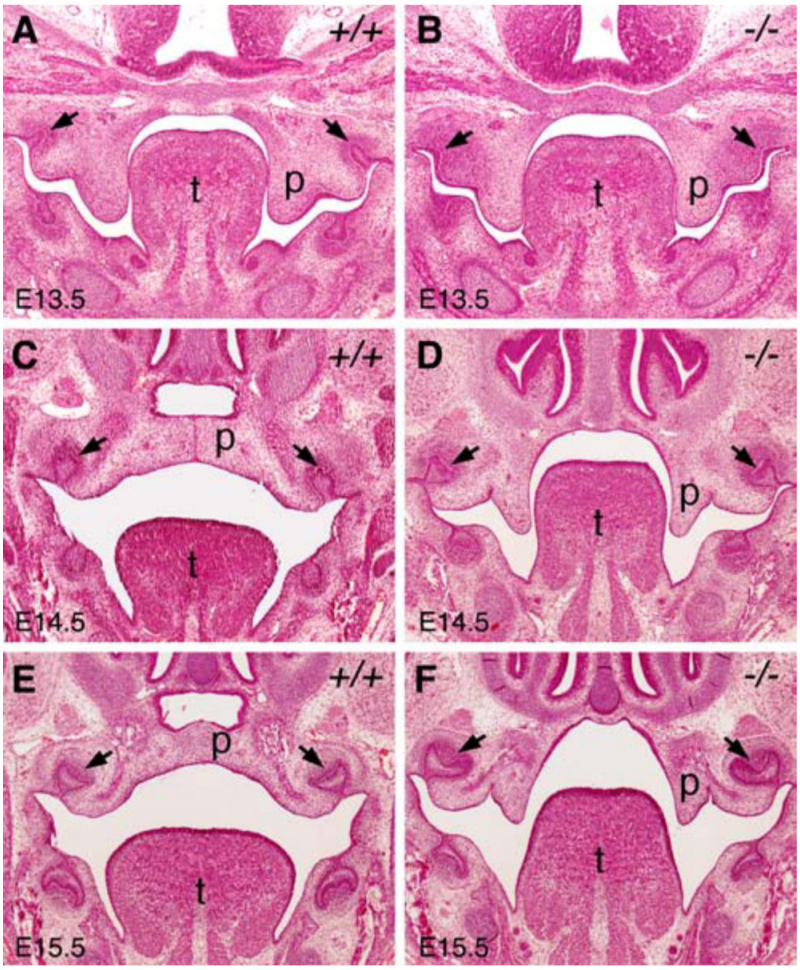

Fig. 3.

Mn1$^{-/-}$ mutant mice exhibit palatal retardation and failure of palatal shelf elevation. All panels shown are from middle palate regions. (A, B) At E13.5, wild-type (A) and *Mn1*$^{-/-}$ homozygous mutant (B) embryos exhibited similar palatal shelf size and shape. (C, D) At E14.5, the wild-type (C) palatal shelves had elevated to the horizontal position above the tongue and initiated fusion by forming the midline epithelial seam, while the *Mn1*$^{-/-}$ homozygous mutant (D) palatal shelves were still vertically oriented. (E, F) At E15.5, the wild-type (E) palatal shelves had completed fusion, but the *Mn1*$^{-/-}$ homozygous mutant (F) palatal shelves remained vertically oriented. Arrows point to the first molar tooth germs. p, palatal shelf; t, tongue.

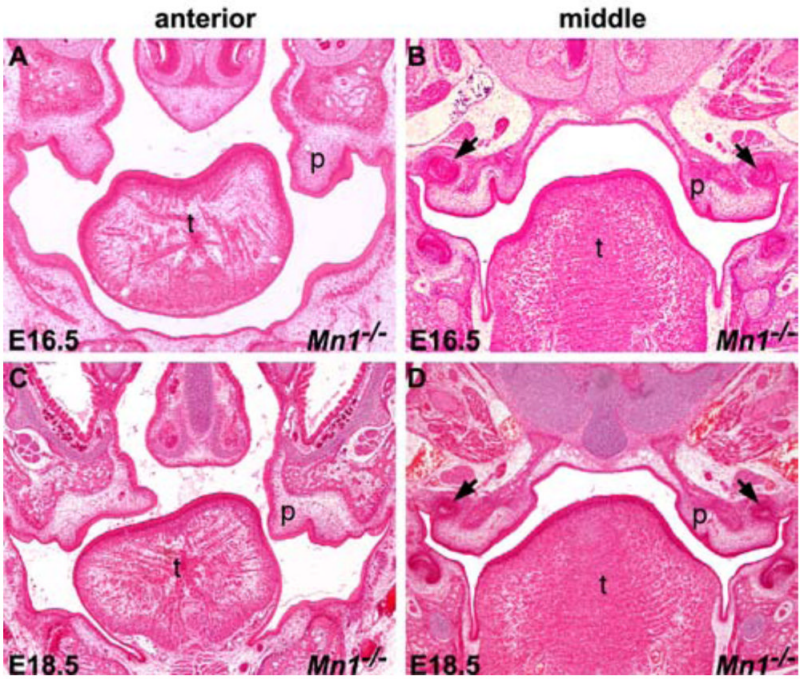

Fig. 4.

Histological analyses of palate development in *Mn1*$^{-/-}$ mutants at late stages. (A, B) At E16.5, the palatal shelves in *Mn1*$^{-/-}$ mutant embryos were still vertically oriented. In addition, the palatal shelves appeared to be significantly diminished in size in the middle to posterior regions (B). (C, D) At E18.5, whereas the palatal shelves in the anterior region in the *Mn1*$^{-/-}$ mutant mice were partially elevated (C), the middle and posterior regions of the palatal shelves were further retarded and retracted into the maxillary processes (D). Arrows in B and D point to the upper first molar tooth germs. p, palatal shelf; t, tongue.

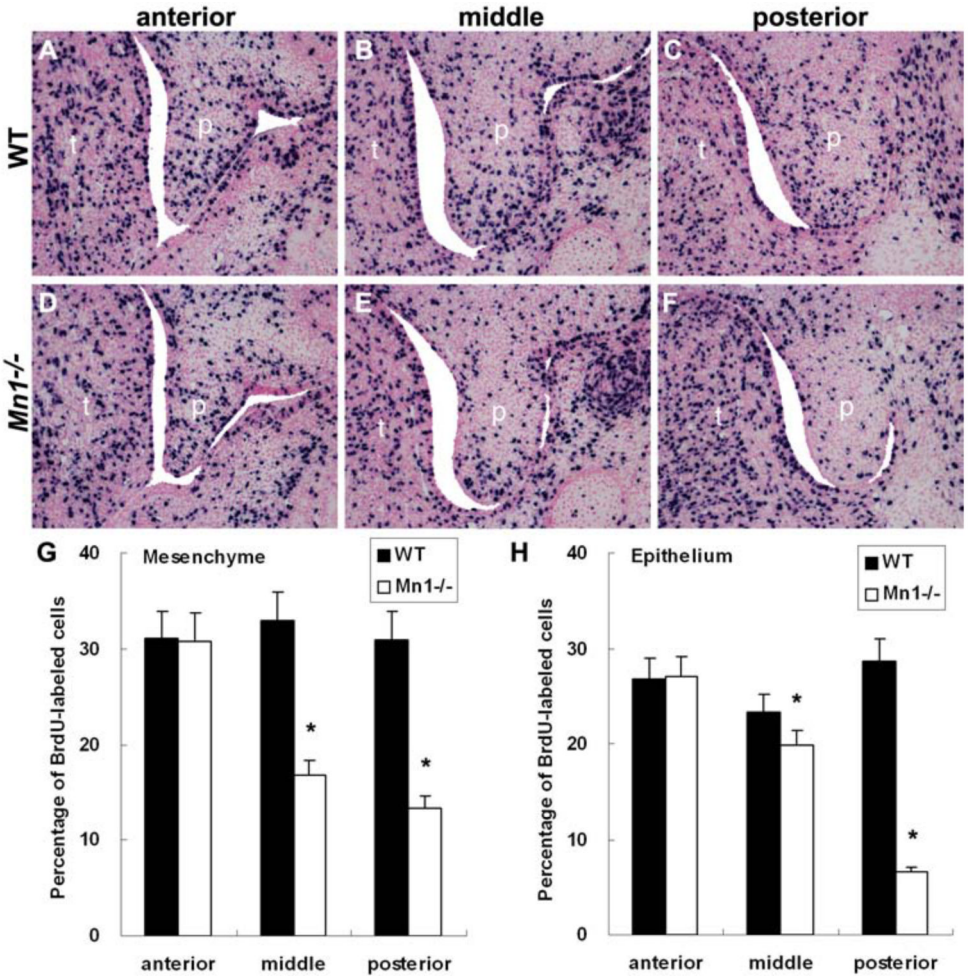

Fig. 5.

Analyses of cell proliferation during palate development in wild-type and *Mn1*$^{-/-}$ mutant embryos. In comparison with the wild-type littermates (A-C), the number of BrdU-labeled cells in the developing palatal shelves was greatly reduced in the middle (E) and posterior (F) palatal shelves, but not in the anterior (D) palatal mesenchyme in the *Mn1*$^{-/-}$ mutant embryos by E13.5. p, palatal shelf; t, tongue. (G, H) Comparison of the percentage of BrdU-labeled cells in the palatal mesenchyme (G) and epithelium (H), respectively, in the anterior, middle, and posterior palatal regions in E13.5 wild-type (WT) and *Mn1*$^{-/-}$ mutant embryos. Error bars represent standard deviation and asterisk denotes a significant difference ($P<0.01$) between the wild-type and *Mn1*$^{-/-}$ mutant samples.

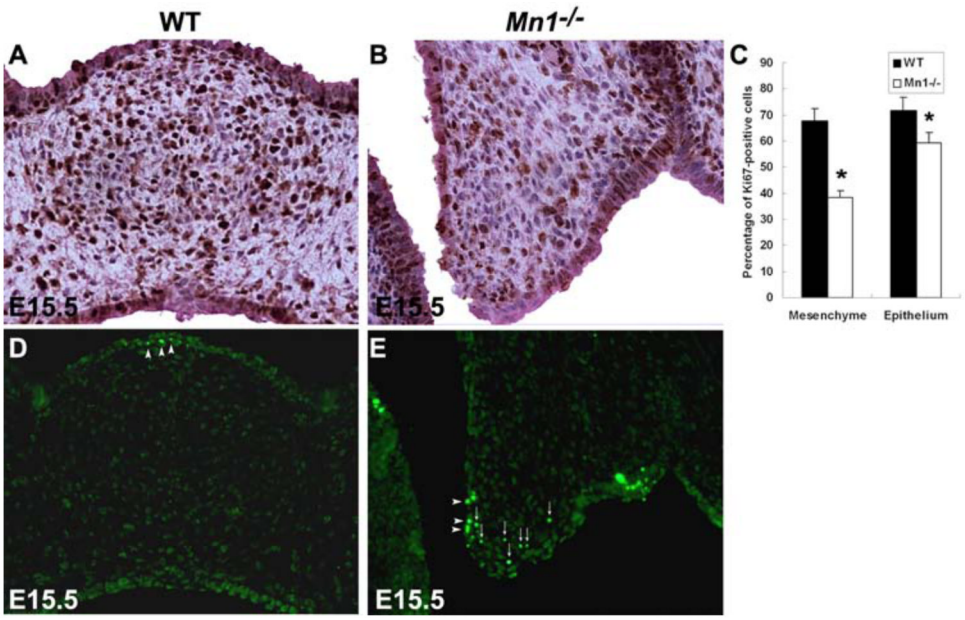

Fig. 6.

Analyses of cell proliferation and cell apoptosis in wild-type (WT) and *Mn1*$^{-/-}$ mutant embryos at E15.5. (A-C) Cell proliferation in palatal mesenchyme detected using immunohistochemical staining of the Ki67 protein. In comparison with wild-type embryos (A), cell proliferation in the middle palatal region in *Mn1*$^{-/-}$ mutant embryos (B) was greatly reduced. Error bars in (C) represent standard deviation and asterisk denotes a significant difference ($P<0.01$) between the wild-type and mutant samples. (D-E) TUNEL assays mid-palatal sections of E15.5 palatal shelves of wild-type (D) and *Mn1*$^{-/-}$ mutant (E) embryos showed increased cell apoptosis in the palatal mesenchyme in the mutant. Small arrows point to highly TUNEL-positive palatal mesenchymal cells and arrowheads point to highly TUNEL-positive palatal epithelial cells.

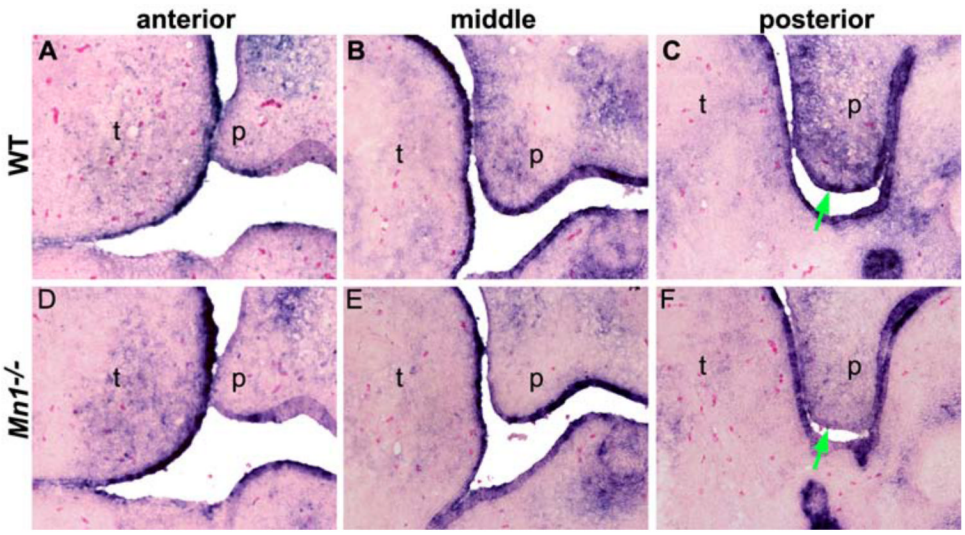

Fig. 7.

Expression of *CyclinD2* was down-regulated in *Mn1*$^{-/-}$ mutant palatal shelves at E13.5. (A,D) In the anterior region of the developing palate, expression of *CyclinD2* was similarly weak in wild-type (A) and *Mn1*$^{-/-}$ mutant (D) embryos. (B,E) In the middle palate, *CyclinD2* is highly expressed in both the epithelium and mesenchyme in the wild-type embryo (B) but its expression is much reduced in the *Mn1*$^{-/-}$ palatal mesenchyme (E). (C) In the posterior palate region, strong *CyclinD2* expression was detected in both the epithelium and mesenchyme in the wild-type palate. (F) In comparison to the wild-type littermate, *CyclinD2* expression is much reduced in both the palatal epithelium and mesenchyme in the posterior palatal region in the *Mn1*$^{-/-}$ mutant embryo. Green arrows in C and F point to the medial edge epithelium of the palatal shelves.

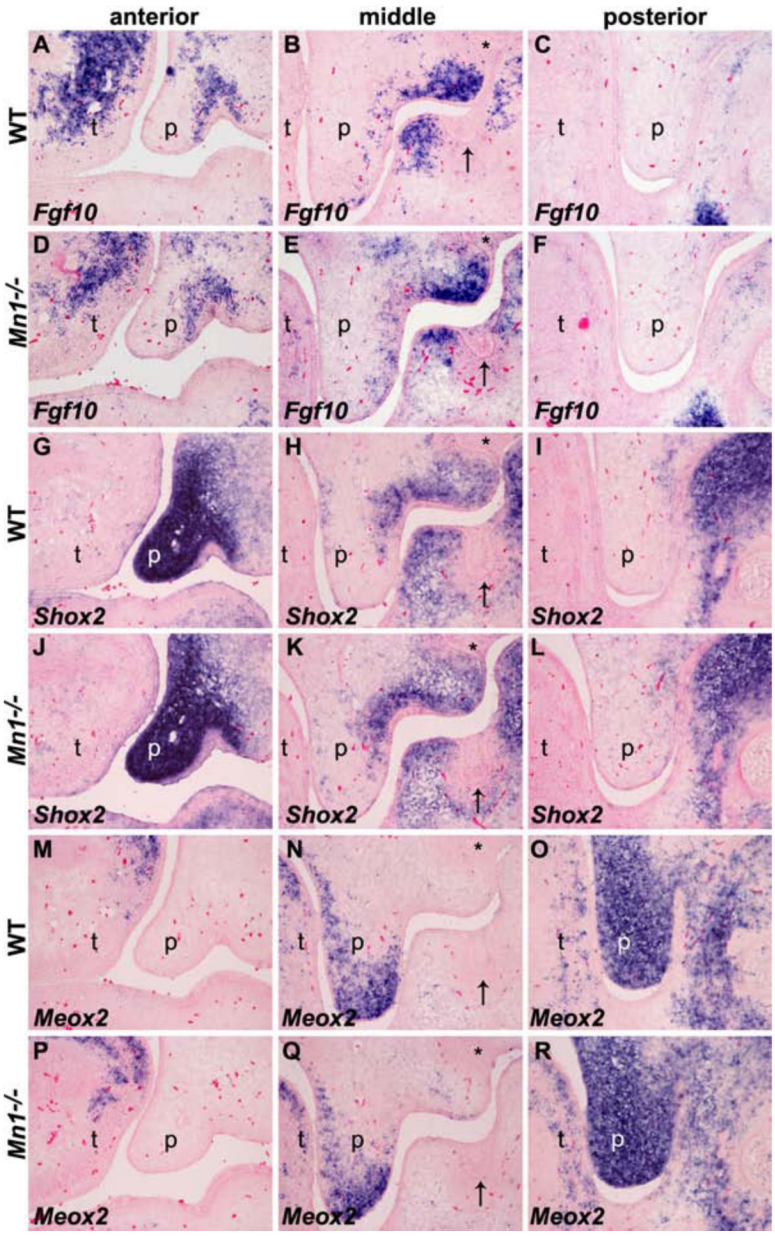

Fig. 8.

The anterior-posterior pattern of the developing palatal shelves is not disrupted in the *Mn1*$^{-/-}$ mutant embryos. (A-F) Expression of *Fgf10* along the anterior-posterior axis of the developing palatal shelves in wild-type (A-C) and *Mn1*$^{-/-}$ mutant (D-F) embryos at E13.5. *Fgf10* showed similar restricted expression pattern in the anterior and middle palatal regions in both wild-type and *Mn1*$^{-/-}$ mutant embryos. (G-L) Expression of *Shox2* along the anterior-posterior axis of the developing palatal shelves in wild-type (G-I) and *Mn1*$^{-/-}$ mutant (J-L) embryos at E13.5. *Shox2* mRNA is strongly expressed in the anterior and absent in the posterior palatal regions in wild-type embryos (G-I). In the middle palate, *Shox2* mRNA expression is restricted in the proximolateral region (H). The expression pattern and levels of *Shox2* mRNA are not altered in *Mn1*$^{-/-}$ mutant (J-L) embryos. (M-O) *Meox2* mRNA expression is restricted to the middle and posterior regions and absent from the anterior region of the developing palate in wild-type embryos at E13.5. (P-R) The levels and anterior-posterior pattern of *Meox2* mRNA expression

pattern in E13.5 *Mn1*$^{-/-}$ mutant embryo are comparable to that of the wild-type littermate (M-O). p, palatal shelf; t, tongue. Arrows point to the mandibular first molar tooth germs and asterisks mark the maxillary first molar tooth germs in the mid-palatal sections.

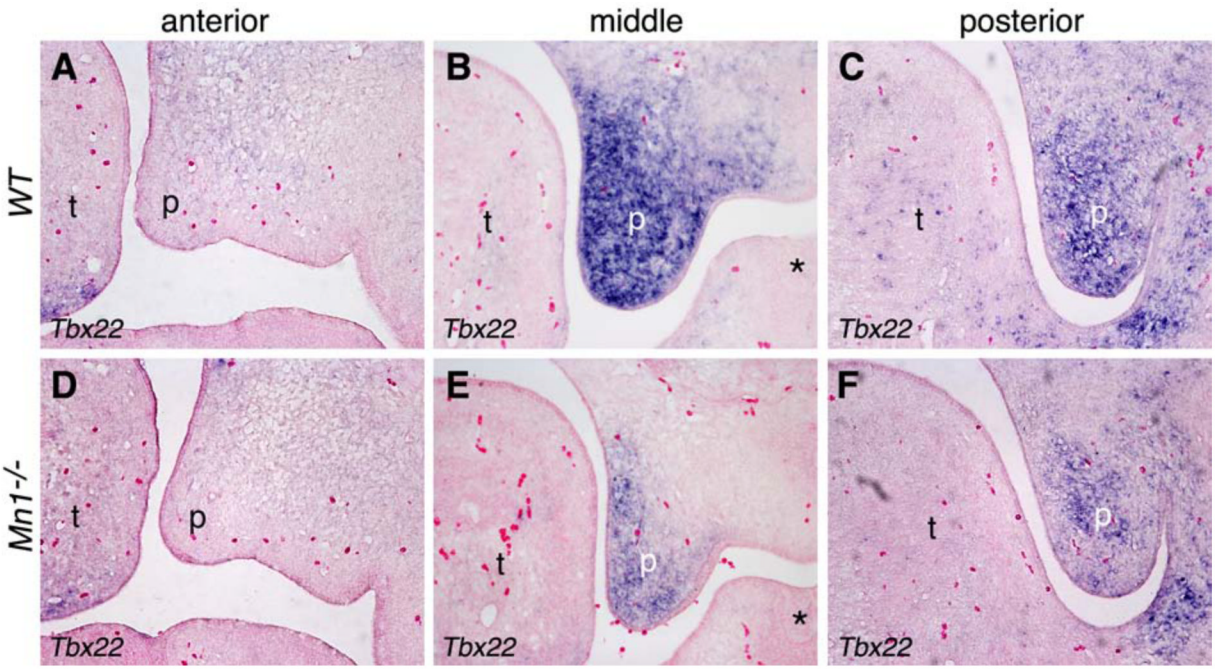

Fig. 9.

Tbx22 is specifically down-regulated in *Mn1*$^{-/-}$ mutant palatal shelves at E13.5. (A-C) *Tbx22* mRNA is strongly expressed in the middle (B) and posterior (C) palatal mesenchyme, but barely expressed in the anterior (A) palatal mesenchyme in wild-type embryos. (D-F) *Tbx22* expression is much reduced in the middle (E) and posterior (F) palatal mesenchyme in the *Mn1*$^{-/-}$ mutant littermates. Asterisk in B and E marks the mandibular first molar tooth germ. p, palatal shelf; t, tongue.

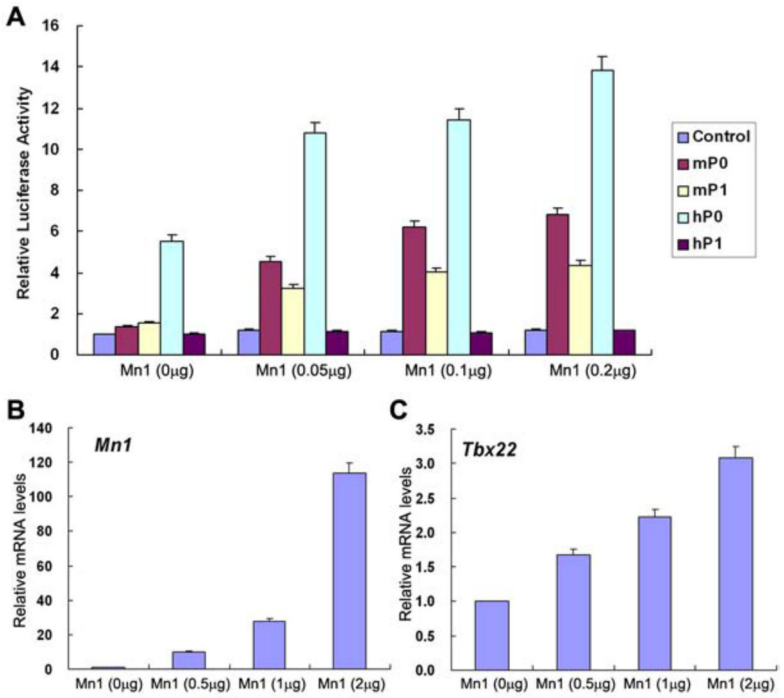

Fig. 10.

Transcriptional regulation of *Tbx22* by Mn1. (A) *Tbx22* promoter-luciferase reporter activity in transfected NIH3T3 cells in the absence or presence of increasing amounts of co-transfected *Mn1* expression vector. Luciferase activity was normalized against the control (promoter-less pGL3-basic) vector transfected cells. Error bar represents standard deviation. (B,C) Effect of *Mn1* overexpression on endogenous *Tbx22* mRNA expression in NIH3T3 cells. Expression levels of *Mn1* (B) and *Tbx22* (C) mRNAs were quantified by real time RT-PCR and normalized against mock-transfected cells. Error bar represents standard deviation.